Article

Not peer-reviewed version

# Conducting and Magnetic Hybrid Polypyrrole/Nickel Composites and their Application in Magnetorheology

Marek Jurča , Jarmila Vilčáková , Natalia E. Kazantseva , Andrei Munteanu , Lenka Munteanu , Michal Sedlačík , Jaroslav Stejskal * , Miroslava Trchová , Jan Prokeš

Posted Date: 28 November 2023

doi: 10.20944/preprints202311.1736.v1

Keywords: nickel microparticles; polypyrrole; hybrid composites; resistivity; conductivity; magnetization; magnetorheology

*Article*

# Conducting and Magnetic Hybrid Polypyrrole/Nickel Composites and Their Application in Magnetorheology

**Marek Jurča [1], Jarmila Vilčáková [1], Natalia E. Kazantseva [1], Andrei Munteanu [1], Lenka Munteanu [1], Michal Sedlačík [1], Jaroslav Stejskal [1,2,*], Miroslava Trchová [2] and Jan Prokeš [3]**

[1] University Institute, Tomas Bata University in Zlín, 760 01 Zlín, Czech Republic; jurca@utb.cz (M.J.); vilcakova@utb.cz (J.V.); kazantseva@utb.cz (N.E.K.); munteanu@utb.cz (A.M.); strouhalova@utb.cz (L.M.); msedlacik@utb.cz (M.S.)

[2] University of Chemistry and Technology, Prague, 166 28 Prague 6, Czech Republic; miroslava.trchova@vscht.cz

[3] Faculty of Mathematics and Physics, Charles University, 180 00 Prague 8, Czech Republic; jprokes@semi.mff.cuni.cz

* Correspondence: stejskal@utb.cz

**Abstract:** Hybrid organic/inorganic conducting and magnetic composites of core–shell type have been prepared by in-situ coating of nickel microparticles with polypyrrole. Three series of syntheses have been made. In the first, pyrrole was oxidized with ammonium peroxydisulfate in water in the presence of various amounts of nickel and the composites contained up to 83 wt% of this metal. The similar syntheses in 0.1 M sulfuric acid followed. Finally, the composites with polypyrrole nanotubes were prepared in water in the presence of structure-guiding methyl orange dye. FTIR and Raman spectroscopies confirmed the formation of polypyrrole. The resistivity of composite powders of the order of tens to hundreds Ω cm was monitored as a function of pressure up to 10 MPa. The resistivity of composites slightly increased with increasing content of conducting nickel. This apparent paradox is explained by the coating of nickel particles, which prevents their contacts and generation of metallic conducting pathways. Electrical properties were practically independent of the way of composite preparation or nickel fraction and were controlled by polypyrrole phase. On the contrary, magnetic properties were determined exclusively by nickel content. The composites were used as a solid phase to prepare a magnetorheological fluid. The test showed better performance when compared with a different nickel system.

**Keywords:** nickel microparticles; polypyrrole; hybrid composites; resistivity; conductivity; magnetization; magnetorheology

## 1. Introduction

Hybrid organic/inorganic composites constitute a core of many functional materials. This applies especially to the cases when both matrix/filler components have a functional character, i.e. they display complementary chemical or physical properties alone or in accord. The combination of metals with conducting polymers is one of the possibilities frequently discussed in the literature in the design of energy conversion and storage devices and variety of other applications. Even though the composites applied in practice often include additional inorganic component, typically mixed metal oxides and sulfides or carbons [1,2], the understanding of binary systems is essential. One of the open research tasks includes the preparation of polypyrrole/nickel composites.

Nickel is a key element used in electrodes for its conductivity and electrocatalytic activity, suitable morphology and materials properties. Furthermore, its magnetic properties make the element even more attractive. Conducting polymers, such as polypyrrole, have often been used as

 doi:10.20944/preprints202311.1736.v1



additives that improve conductivity, electrochemical activity, and facilitate electron–ion transfers [2]. They can also be used as functional adsorbents in water-pollution treatment. The system composed of metallic nickel and a conducting polymer, polypyrrole, is discussed below.

Nickel metal may be present in two forms, as a nickel foam, or as fibres and microparticles, the former being dominating, the latter more interesting. Nickel foam has been used as a support for the deposition of polypyrrole by the in-situ chemical oxidation of pyrrole with ammonium peroxydisulfate [3–5]. An original approach is represented by the chemical oxidation using silver nitrate [6] at nickel foam that catalysed the pyrrole polymerization and introduced metallic silver at the same time [7]. The polypyrrole coating was obtained in acidic solution even with an added oxidant [8]. In another case, the separately prepared polypyrrole suspension was simply deposited at nickel foam [9]. As an alternative, the nickel foam has been coated with polypyrrole potentiostatically [10,11], at constant current density [12] or by cyclic voltammetry [13,14]. Systems based on nickel foam are applicable especially as current collectors in supercapacitors where the nickel provides the conductivity as well as the mechanical support for the deposition of polypyrrole [4–9,15–17]. Other diverse applications are represented by electrodes for electrocatalytic oxidation of methanol [11], improved water-splitting [14], in solar steam-generation [3,10], solar-thermal desalination [18] or allowed for controlled electrosorption of organic pollutant dye [12].

There are two types of the composites based on polypyrrole and nickel microparticles. The first is represented by the deposition of nickel on conducting polymer. Polypyrrole was electrochemically prepared on graphite electrode followed by the electrochemical electrodeposition of nickel microparticles [19–21]. This type of polypyrrole/nickel particulate composites have been used as the electrocatalyst of hydrogen evolution reaction [17,19] or ethanol oxidation [20], and in the design of glucose biosensor [21] or insulin sensor [22]. The reverse strategy relies on the coating of nickel particles with polypyrrole. Polypyrrole was electrodeposited on nickel particles at silicon nanowire arrays [16]. The chemical oxidation of pyrrole with sodium peroxydisulfate in the presence of nickel flakes is another example [23]. The composite particles improved the conductivity of composites when dispersed in polyethylene matrix compared with neat nickel.

The preparation of polypyrrole-coated nickel microparticles is still a challenge. Virtually any interface immersed in the aqueous reaction mixture used for the preparation of conducting polymers by the chemical oxidation of respective monomers becomes coated with a thin submicrometre polymer film. This applies both for polyaniline and polypyrrole. Such approach has been used for the coating of inorganic particles, e.g., tungsten disulfide [24]. When applied to particles of non-noble metals, such as nickel, some problems have been reported. The oxidation of pyrrole to polypyrrole proceeds invariably in acidic medium. The combination of acidic medium and the presence of an oxidant is expected to cause the corrosion of non-noble metals followed by their dissolution instead of being coated with a conducting polymer. For this reason, studies in this directions have been rare [23,25].

For example, when aniline hydrochloride was oxidized with ammonium peroxydisulfate in the presence of nickel microparticles, polyaniline/nickel was produced at reduced yield and conductivity of the order $10^{-2}$–$10^{-3}$ S $cm^{-1}$, i.e. values below the conductivity of both components alone [25]. This phenomenon was explained by the nickel dissolution assisted by generated sulfuric acid. It was accompanied by the generation of hydrogen gas catalysed by nickel and followed by a simultaneous reduction of emeraldine form of polyaniline to leucoemeraldine. The present study observes the similar trends in polypyrrole/nickel composites but offers alternative explanation.

Polypyrrole/nickel composites, where nickel core is coated with polypyrrole shell, may find use in various electrodes, suspensions in magnetorheology, magnetically separable adsorbents, electrocatalysts, fillers in functional flexible composites, and electromagnetic interference shielding, thus exploiting also magnetic and catalytic properties of nickel. The preparation of such composites is one of the aims of the present study, which also introduces a novel way to deposit polypyrrole nanotubes [26] on nickel.

 doi:10.20944/preprints202311.1736.v1



## 2. Experimental

### *2.1. Preparation*

Nickel microparticles with a hedgehog-like morphology were employed as a conducting and magnetic filler to prepare polypyrrole-coated nickel microparticles. Nickel particles (99.8%; Goodfellow, London, UK) exhibited a normal size distribution with a mean diameter 5.5±1.8 μm. Various amounts of nickel were dispersed in aqueous solution of pyrrole, and then the solution of ammonium peroxydisulfate in water or 0.1 M sulfuric acid was added under stirring to initiate the in-situ polymerization of pyrrole. The concentrations of reactants were 0.1 M pyrrole (1.34 g per 200 mL) and 0.125 M ammonium peroxydisulfate (5.71 g per 200 mL). The polymerization was left to proceed for 30 min at room temperature. The resulting composite microparticles of globular polypyrrole deposited on nickel were separated by filtration, rinsed several times with distilled water or acid solution, followed by ethanol, to remove any unreacted reagents or by-products. The solids were left to dry at ambient temperature in open air for 48 h. The preparation of similar composite of polypyrrole nanotubes and nickel followed the same protocol in water that contained in addition 0.004 M methyl orange (260 mg per 200 mL). All chemicals were supplied by Sigma-Aldrich branch (Prague, Czech Republic) and used as delivered.

### *2.2. Composition*

The composition of the prepared materials involved the combustion of the organic component in oxygen atmosphere at 800 °C in a muffle furnace (Nabertherm L9/S27, Lilienthal, Germany). Additionally, a subset of randomly selected samples was subjected to thermogravimetric analysis (TA Q500; TA Instruments, Eden Prairie, MN, USA) with a heating rate of 10 °C $min^{-1}$ in oxygen atmosphere. The results were consistent with those obtained by bulk combustion method. The residual mass represented by nickel(II) oxide was recalculated to nickel metal.

### *2.3. Morphology*

Scanning electron microscope (Nova NanoSEM FEI, Brno, Czech Republic) was used to assess the morphology of polypyrrole and its composites with nickel. Prior to analysis, the materials were gold sputter-coated using a JEOL JFC 1300 Auto Fine coater (JEOL, Tokyo, Japan).

### *2.4. Spectroscopy*

ATR FTIR spectra were analysed with a Nicolet 6700 spectrometer (Thermo-Nicolet, Waltham, MA, USA) equipped with a reflective ATR extension GladiATR (PIKE Technologies, Fitchburg, WI, USA) and a diamond crystal. Spectra were recorded in the range of 4000–400 $cm^{-1}$ with a resolution 4 $cm^{-1}$, 64 scans, and Happ-Genzel appodization. The OMNIC package was used for both the spectrometer control and spectral data processing.

Dispersive Raman spectra were recorded in a back-scattering geometry using a Scientific DXR Raman microscope (Thermo Fisher Scientific, Waltham, MA, USA) using a 780 nm excitation laser line. The scattered light was analysed by a spectrograph with holographic grating 1200 lines $mm^{-1}$ and a 50 μm pinhole width. The acquisition time was 10 s with 10 repetitions.

### *2.5. Resistivity*

A four-point van der Pauw method using a lab-made press based on a cylindrical glass cell with an inner diameter of 10 mm was used to assess electrical properties [27]. The powdered composites were placed between a support and a glass piston with four wire electrodes fixed at its perimeter. The experimental set-up included a current source a Keithley 220, a Keithley 2010 multimeter and a Keithley 705 scanner with a Keithley 7052 matrix card (Keithley Instruments Inc., Cleveland, OH, USA). The pressure up to 10 MPa (=102 kp $cm^{-2}$) was registered with a L6E3 strain gauge cell (Zemic Europe BV, Etten-Leur, The Netherlands). The pressure was applied with an E87H4-B05 stepper motor (Haydon Switch & Instrument Inc., Waterbury, CT, USA). The sample thickness was recorded

 doi:10.20944/preprints202311.1736.v1



during the compression with a dial indicator Mitutoyo ID-S112X (Mitutoyo Corp., Sakado, Japan). The resistivity was also separately determined on composite pellets prepared after compression at 527 MPa by a manual hydraulic press (Specac, Orpington, UK).

### *2.6. Magnetic Properties*

The magnetic characteristics were determined by measurement of magnetic hysteresis curve in the range ±10 kOe by a vibrating sample magnetometer (VSM, Model 7407, Westerville, OH, USA).

### *2.7. Magnetorheology*

The fluids were prepared by mixing the polypyrrole/nickel composites with a mineral oil (Sigma-Aldrich, Czech Republic; viscosity 19.6 mPa s at 25 °C) at 9 wt% composite content. After preparation and before each measurement, the suspensions were sonicated in ultrasonic bath for 10 min to remove any agglomerates. For the rheological measurements the rotational rheometer Physica MCR 502 (Anton Paar, Graz, Austria) was used. To determine the flow properties of the samples under external magnetic field, the device was equipped with a MRD 170/1T magneto cell and H-PTD hood. Magnetic fields were varied from 0 to 1050 kA $m^{-1}$. For the tests, a 20 mm plate–plate geometry with a sandblasted surface was used to reduce the potential wall slip. The measurements were performed at 300 μm gap and 25 °C, which was controlled using an external bath. Two types of flow tests were performed. At first, the flow curves were obtained for various magnetic fields. The shear rate window used was determined to be between 0.01 and 150 $s^{-1}$ to avoid overflow. The second type of measurement included a step-wise increase of the magnetic field under steady shear. The magnetic field was turned on and off periodically every 20 s while the magnetic field linearly increased by 150 kA $m^{-1}$ with the shear rate kept constant at 50 $s^{-1}$. Before each measurement, the samples were redispersed under shear rate of 50 $s^{-1}$ for 1 min and, after each test, the magnetic field was set to 150 kA $m^{-1}$ to avoid potential sedimentation. Each measurement was repeated at least twice.

## 3. Results and Discussion

### *3.1. Preparation*

It should be noted that polymers chemists invariably use iron(III) chloride as an oxidant of pyrrole due to the superior conductivity of polypyrrole especially in the preparation of polypyrrole nanotubes [26]. When pyrrole was oxidized with iron(III) chloride in the presence of nickel microparticles, however, nickel dissolved and no composite was obtained. In attempt to reduce the acidity of the reaction medium, the oxidant was replaced by ammonium peroxydisulfate. There is a single report in the literature when polypyrrole coating of nickel flakes was achieved by admicellar polymerization of pyrrole, i.e. by the oxidation of pyrrole with sodium peroxydisulfate in the presence of anionic surfactant micelles [23]. The conductivity of coated nickel has not changed and nickel has not dissolved either. When used in polyethylene matrix, improved particle contacts afforded by polypyrrole coating were found. Following this approach, pyrrole was oxidized with ammonium peroxydisulfate in aqueous medium along with various portions of nickel microparticles, and conducting polypyrrole/nickel composites have been obtained in stoichiometric yield (Figure 1). In the contrast to the case of polyaniline [25], no hydrogen evolution associated with a partial metal dissolution of nickel has been observed.

Preprints (www.preprints.org) | NOT PEER-REVIEWED | Posted: 28 November 2023 doi:10.20944/preprints202311.1736.v1



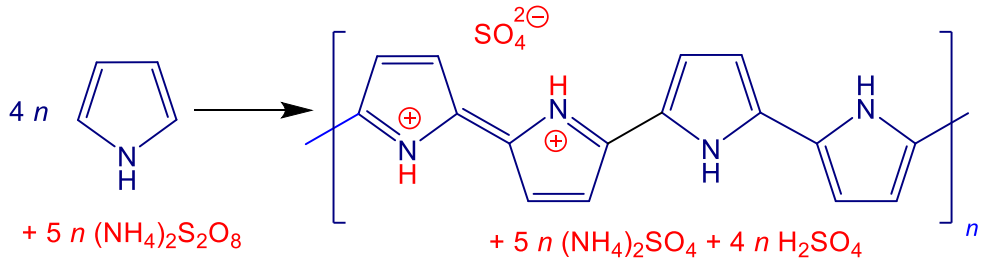


**Figure 1.** The oxidation of pyrrole with ammonium peroxydisulfate yields polypyrrole (sulfate salt). Ammonium sulfate and sulfuric acid are by-products.

In the present synthesis, 20 mmol (1.34 g) of pyrrole is oxidized witth ammonium peroxydisulfate (5.71 g) in 200 mL of aqueous medium. The idealized stoichiometry (Figure 1) thus expects the 1.78 g yield of polypyrrole sulfate. There is some uncertainty in this estimate because the presence of hydrogen sulfate counter-ions instead of sulfate ones has not been considered. Various amount of nickel, 0.5–8 g, were introduced prior to oxidant addition. The composite yields were close to each other in all three series carried out (1) in 0.1 M sulfuric acid, (2) in water, and (3) in water in the presence of methyl orange (MO). The compositions were practically independent of reaction medium and well corresponded to the stoichiometric expectation (Table 1). Both components of composite differ in density, 1.5 g $cm^{-3}$ for polypyrrole [28] and 8.91 g $cm^{-3}$ for nickel at 20 °C. One should keep in mind that for the electrical properties are controlled by volume fractions of components and volume fractions of nickel are considerably lower than those based on weight (Table 1).

**Table 1.** Composite composition expected from the reaction stoichiometry (Figure 1) in dependence on nickel entering to 200 mL of reaction mixture, and the nickel content found in the composites prepared in acidic medium or in water (globular polypyrroles), and in water in the presence of methyl orange (polypyrrole nanotubes).

| Nickel, | Expected nickel content | | Nickel content found, wt% | | |
|---|---|---|---|---|---|
| g/200 mL | wt% Ni | vol% Ni | 0.1 M $H_2SO_4$ | Water | Water+MO |
| 0.5 | 21.9 | 4.5 | – | 18.3 | 22.9 |
| 1 | 36.0 | 8.7 | – | 35.0 | 33.6 |
| 2 | 52.9 | 15.9 | 52.8 | 56.4 | 53.1 |
| 4 | 69.2 | 27.4 | 70.2 | 70.9 | 70.7 |
| 6 | 77.1 | 36.2 | 77.7 | 78.5 | 78.3 |
| 8 | 81.2 | 42.1 | 84.7 | 83.2 | 83.4 |

*3.2. Morphology*

Nickel microparticles have typical hedgehog morphology (Figure 2a) with the size of several micrometres and medium polydispersity. Polypyrrole was prepared without and with methyl orange, respectively. The former reveals the typical globular morphology with a particle size 50–200 nm (Figure 2b), the latter resulted in the formation of polypyrrole nanotubes accompanied with a significant fraction globular morphology (Figure 2c). It has to be stressed that uniform and highly conducting polypyrrole nanotubes are prepared with iron(III) chloride oxidant and its replacement with ammonium peroxydisulfate in present study led to definitely inferior morphology with only a sporadic occurrence of nanotubes.

Preprints (www.preprints.org) | NOT PEER-REVIEWED | Posted: 28 November 2023 doi:10.20944/preprints202311.1736.v1



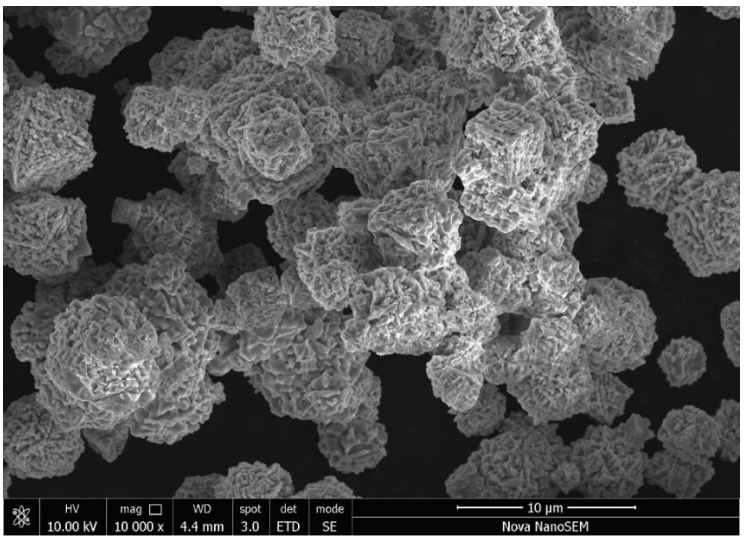


(**a**) Nickel microparticles

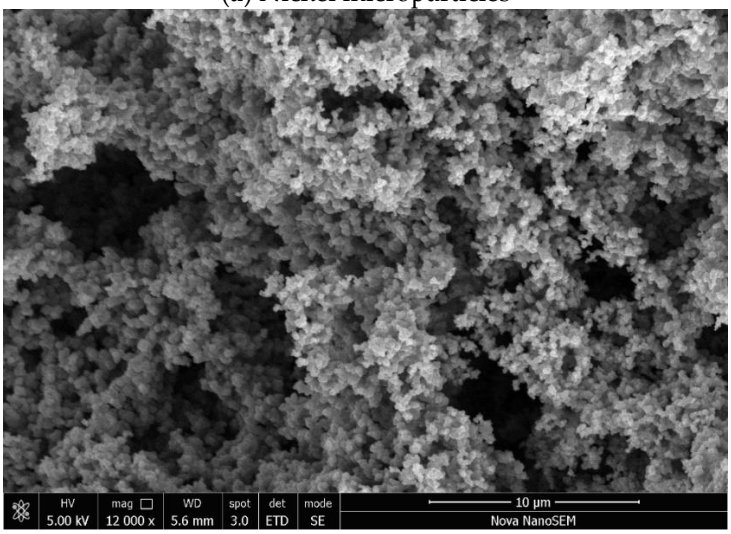


(**b**) Globular polypyrrole

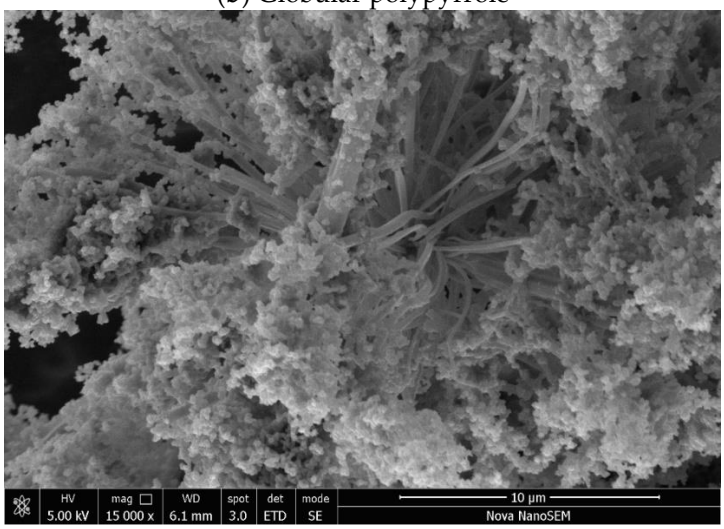


(c) Polypyrrole nanotubes

**Figure 2.** Scanning electron micrographs of composite components: (a) nickel and (b) globular polypyrrole, and (c) polypyrrole nanotubes/globules.

The images of polypyrrole/nickel composites show only the presence of polypyrrole in globular form (Figure 3a) or its mixture with polypyrrole nanotubes with a diameter of about 100–500 nm and a length of 5–10 µm (Figure 3b). No nickel microparticles are observed. During the polypyrrole

Preprints (www.preprints.org) | NOT PEER-REVIEWED | Posted: 28 November 2023 doi:10.20944/preprints202311.1736.v1



synthesis, this polymer grows at the nickel surface resulting in complete coating of metal microparticles. As a result, nickel particles are dispersed in the polypyrrole matrix and they stay apart from each other within the polymer phase. Such composite structure determines the electrical properties discussed below.

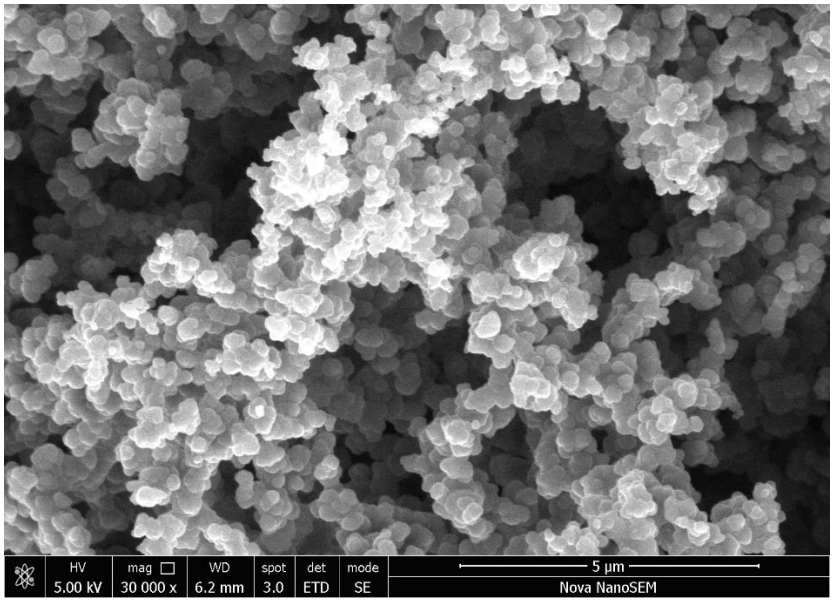


(**a**) Globular polypyrrole/nickel

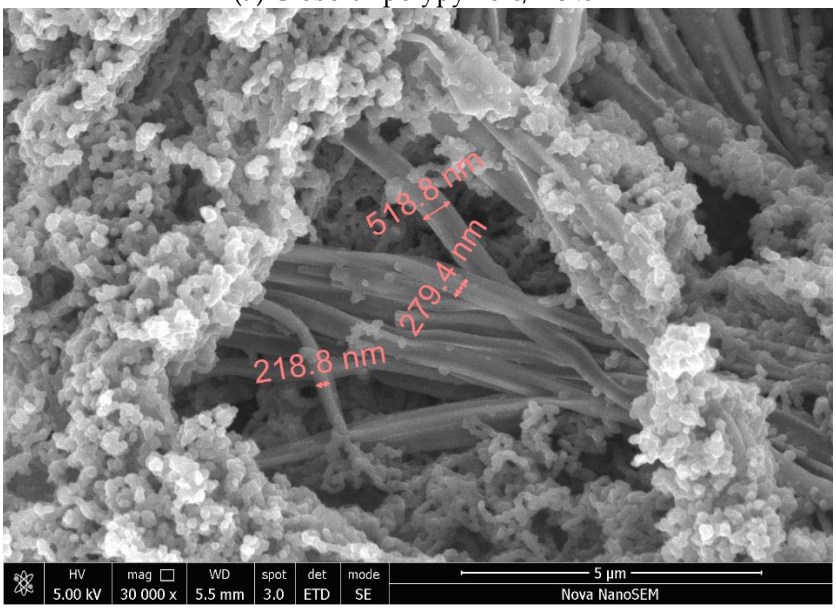


(**b**) Polypyrrole nanotubes/nickel

**Figure 3.** Scanning electron micrographs of composites (ca 50 wt% nickel) for (a) polypyrrole globules and (b) nanotubes deposited on nickel.

*3.3. Spectroscopy*

ATR FTIR spectrum of powdered polypyrrole prepared in absence of nickel (PPy in Figure 4) corresponds to the protonated form of polypyrrole (Figure 1), which exhibits, in addition to a broad absorption band at wavenumbers above 2000 $cm^{-1}$ (not shown in the Figure), the main bands with local maxima situated at 1542 $cm^{-1}$ (C–C stretching vibrations in the pyrrole ring), 1467 $cm^{-1}$ (C–N stretching vibrations in the ring), 1290 $cm^{-1}$ (C–H and C–N in-plane deformation modes), 1164 $cm^{-1}$ (breathing vibrations of the pyrrole ring), 1094 $cm^{-1}$ (breathing vibrations of pyrrole ring), 1036 $cm^{-1}$ (C–H and C–N in-plane deformation vibrations), 991 $cm^{-1}$ (C–H out-of-plane deformation vibrations of the ring), and at 897 $cm^{-1}$ (C–C out-of-plane deformation vibrations of the ring) [26]. The maximum

Preprints (www.preprints.org) | NOT PEER-REVIEWED | Posted: 28 November 2023 doi:10.20944/preprints202311.1736.v1



of the broad band detected at 1686 $cm^{-1}$ was assigned to the presence of carbonyl group previously attributed to the nucleophilic attack of water on pyrrole ring during the preparation [26]. The shape of polypyrrole spectra did not change with increasing amount of nickel in the reaction mixture, i.e. nickel does not interfere with the formation of polypyrrole. A small shift of the maxima of the main bands to higher wavenumbers may indicate a slight deprotonation of the polypyrrole with increasing amount of nickel. There is no observable difference between polypyrrole prepared in water of in 0.1 M sulfuric acid (Figure 4). This is not surprising because sulfuric acid is generated as a by-product during the synthesis (Figure 1).

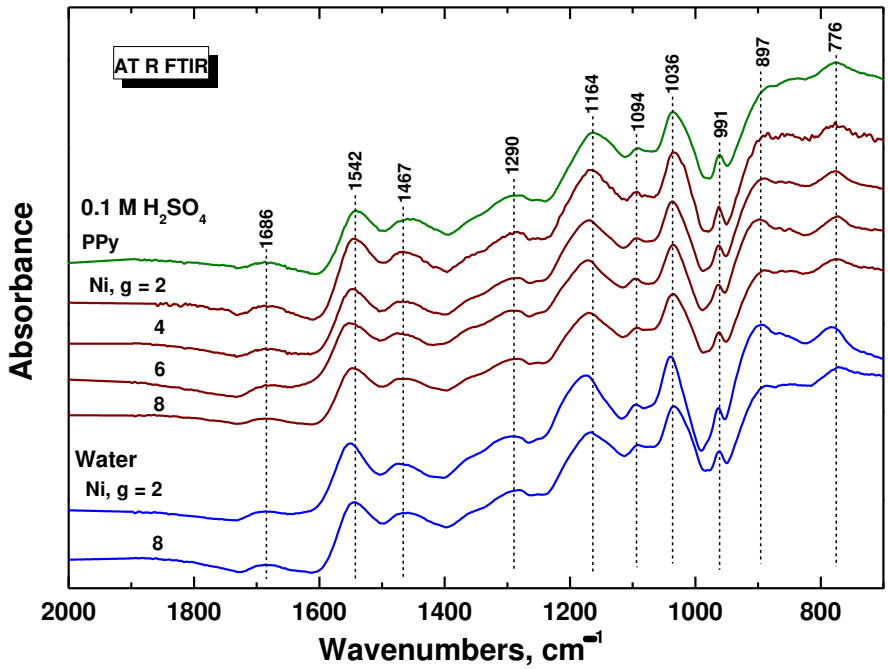


**Figure 4.** ATR FTIR spectra of polypyrrole and polypyrrole/nickel composites (2–8 g nickel) prepared in 0.1 M sulfuric acid or in water.

Raman spectroscopy is the surface dedicated method. In Raman spectra of polypyrrole prepared in the absence of nickel (PPy in Figure 5), we detect the bands of polypyrrole with local maxima at 1590 $cm^{-1}$ (C=C stretching vibrations of polypyrrole backbone) and 1479 $cm^{-1}$ (C–C and C=N stretching skeletal vibrations), two bands of ring-stretching vibrations at 1382 and 1315 $cm^{-1}$, a band at 1245 $cm^{-1}$ (antisymmetric C–H deformation vibrations), and a double-peak with local maxima at 1085 and 1045 $cm^{-1}$ (C–H out-of-plane deformation vibrations, the second became sharper during deprotonation [29]). This is in agreement with the infrared spectra that suggest a slight deprotonation of the samples with increasing of the amount of nickel.

Preprints (www.preprints.org) | NOT PEER-REVIEWED | Posted: 28 November 2023 doi:10.20944/preprints202311.1736.v1



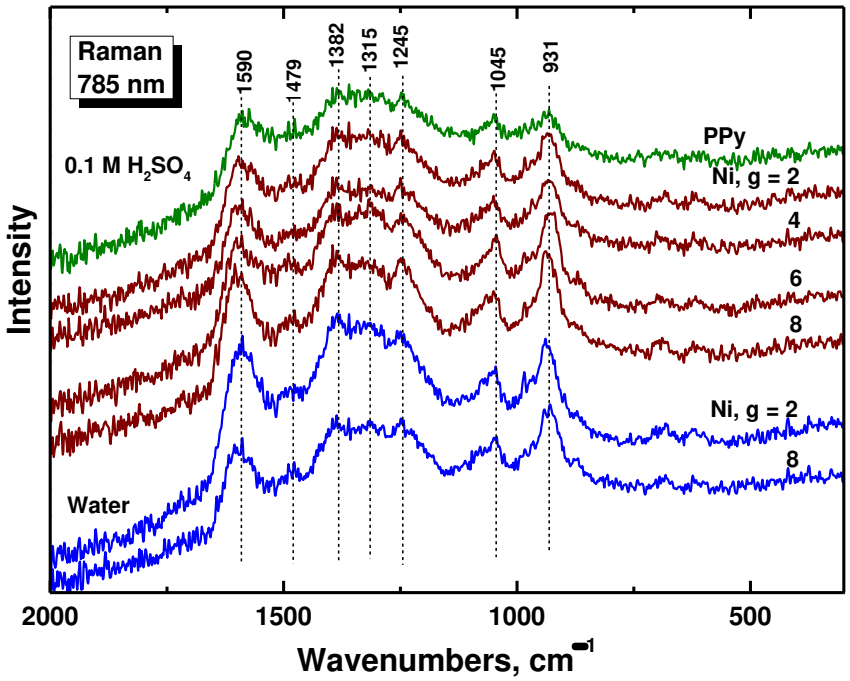


**Figure 5.** Raman spectra of polypyrrole (PPy) and polypyrrole/nickel composites (Ni, g = 2–8) prepared in water and in 0.1 M sulfuric acid.

*3.4. Resistivity*

The resistivity of various conducting powders is usually determined by four-point method on compressed pellets. For many samples, free-standing pellets cannot be prepared, e.g., carbon black or carbon nanotubes, nickel or ferrite microparticles, being examples and the characterization has to be performed under applied pressure. This is not the case of present composites but the measurement of pressure dependences of resistivity provides additional information about electrical properties of powders.

Double-logarithmic dependences of resistivity on pressure are linear in the investigated range 0.1–10 MPa for composites of both types of polypyrrole with nickel (Figure 6a,b). The resistivity of neat nickel particles recorded in the same manner is two orders of magnitude lower (Figure 6c). When compressed at 10 MPa, it was $1.43\times10^{-3}$ Ω cm, which corresponds to 700 S $cm^{-1}$ conductivity, in the accordance with the earlier results [25]. The results then constitute an apparent paradox illustrating that the introduction of highly conducting nickel results in the *increase* of resistivity and this becomes even more pronounced as the nickel content grows.

Preprints (www.preprints.org) | NOT PEER-REVIEWED | Posted: 28 November 2023 doi:10.20944/preprints202311.1736.v1



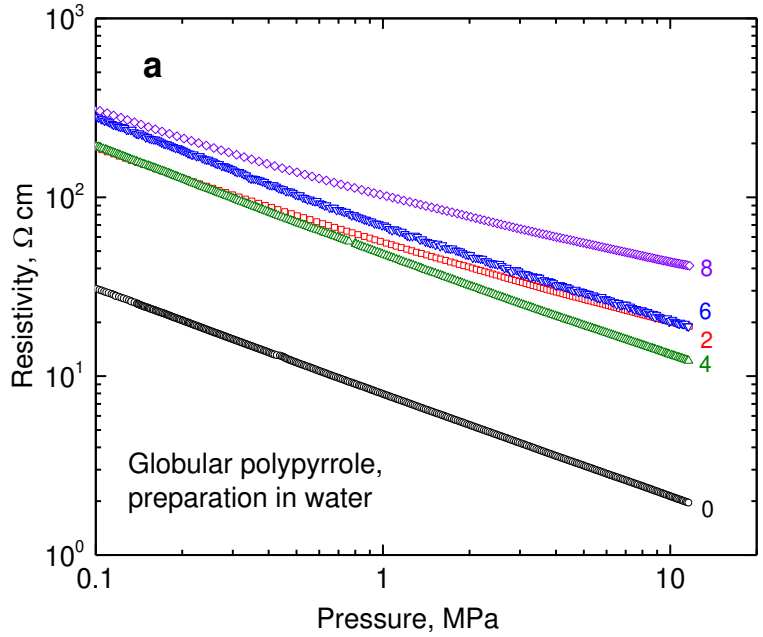


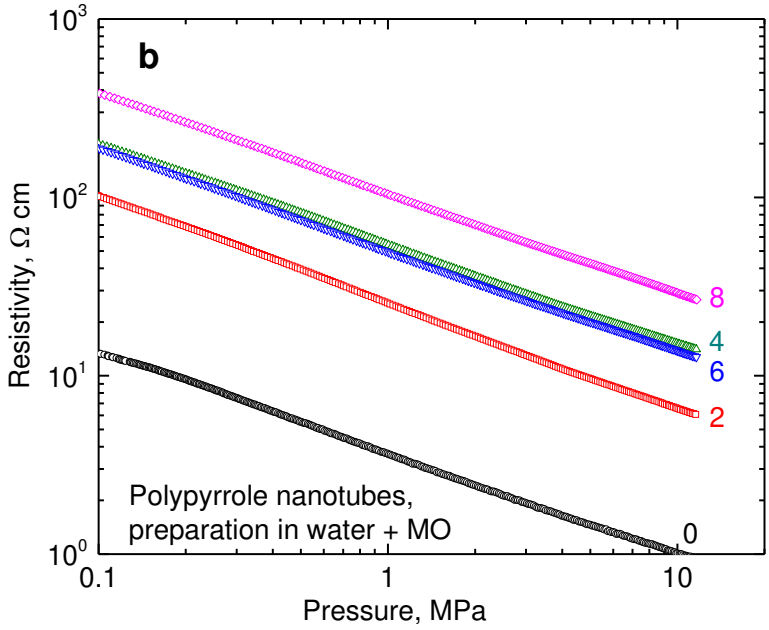

Preprints (www.preprints.org) | NOT PEER-REVIEWED | Posted: 28 November 2023 doi:10.20944/preprints202311.1736.v1



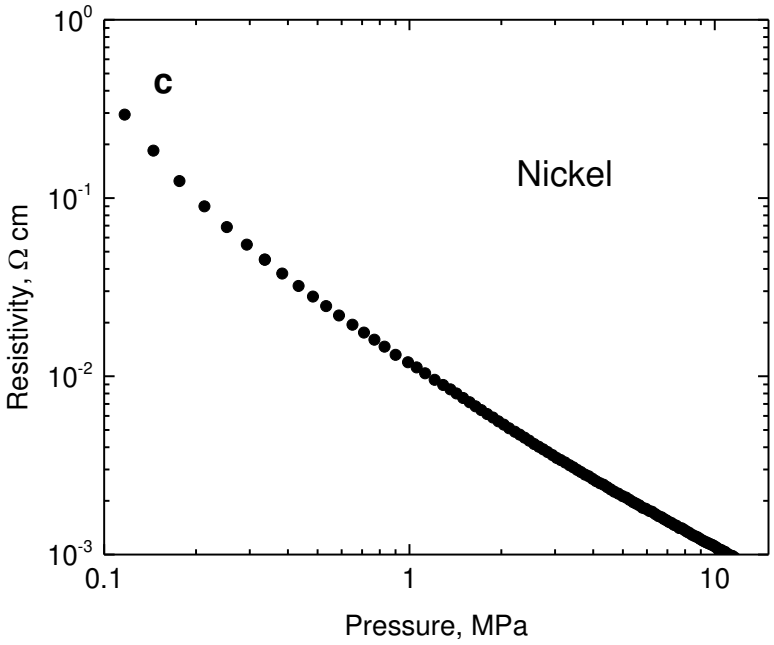


**Figure 6.** The pressure dependence of resistivity for (a) globular polypyrrole (0) and its polypyrrole/nickel composites (2–8 g nickel) and (b) for analogous polypyrrole nanotubes and their composites with nickel. (c) The similar dependence for neat nickel microparticles.

The explanation follows: Let us consider the classical case when the conducting metal particles are gradually introduced into a non-conducting polymer matrix. When their fraction is low, they are randomly distributed without any mutual contacts. In such composite, no conducting pathways are present, and the composite would remain non-conducting despite the presence of dispersed conducting objects. When the content of metal particles becomes higher, their contacts start to occur and finally they generate the first conducting pathway at so-called percolation threshold. The conductivity then starts to grow rapidly with increasing metal content.

The microstructure of the system under study, however, is different. Instead of neat metal particles distributed in the polymer matrix, the composite is constituted by metal particles *coated* with polypyrrole. This coating and any accompanying polypyrrole forms the conducing matrix. This means that the coating prevents the contacts between metal particles, they will always be separated regardless of their fraction, they cannot therefore create any conducting pathways, and thus contribute to the overall composite conductivity. The conductivity of the composite is thus determined by the conductivity of polypyrrole matrix.

In addition, as the content of metal particles in the composite increases, the volume fraction of matrix decreases accordingly and, consequently, the resistivity of composite increases (Figure 6a,b). Such results produce an apparent paradox when the increasing introduction of conducting metal particles (but coated with polymer!), leads to the increase in the composite resistivity. The similar behaviour has earlier been observed with nickel microparticles coated with polyaniline [25].

*In the present case, the standard compact pellets can also be prepared by compression at 527 MPa. The resistivity determined with them is several times lower than that found at 10 MPa pressure (Figure 7a). The resistivity of true polypyrrole nanotubes is lower compared with globular polypyrrole [26] but, in the present study, the nanotubular morphology has not been fully developed. As far as the composites are concerned, the conductivity is therefore about the same within the order of magnitude regardless of the way of preparation and polypyrrole morphology.*

Some readers may prefer plotting the conductivity against the volume fraction of nickel (Table 1, Figure 7b). The apparent paradox demonstrated then by the decrease in composite conductivity with increasing content of highly conducting nickel microparticles is obvious.

Preprints (www.preprints.org) | NOT PEER-REVIEWED | Posted: 28 November 2023 doi:10.20944/preprints202311.1736.v1



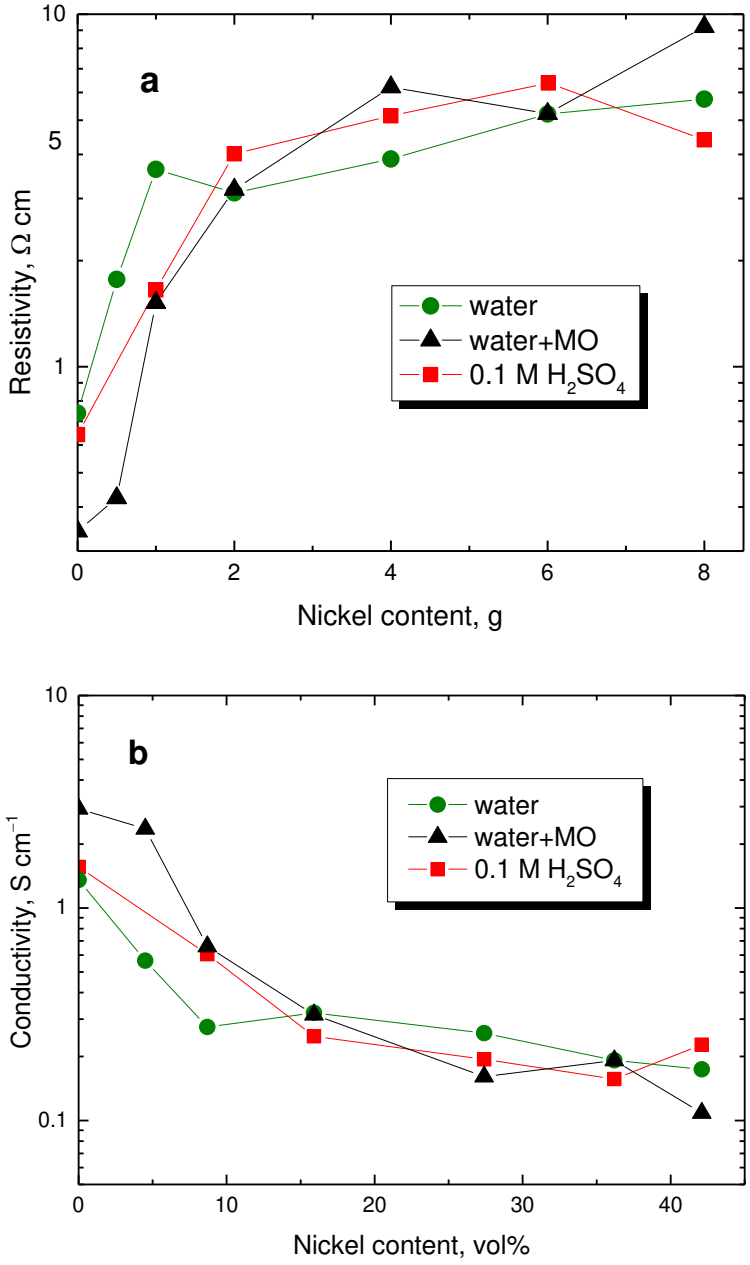


**Figure 7.** (a) Resistivity of polypyrrole/nickel composites determined in pellets in dependence on nickel content (in g) and (b) its reciprocal value, conductivity, on nickel content (in vol%). Preparation of globular polypyrrole in water (circles), nanotubes in the presence of methyl orange (tringles), or in acidic medium (squares).

*3.5. Mechanical Properties*

The experimental set-up used for the determination of resistivity allows also for the monitoring of sample thickness during the compression (Figure 8). The pressure dependence of composites is close to linear in double-logarithmic presentation. The slope provides information about the fluffiness, i.e. the steeper it is, easier the material is compressed. The decrease in the slope with increasing nickel content reflects the composite reinforcement with metallic microparticles.

Preprints (www.preprints.org) | NOT PEER-REVIEWED | Posted: 28 November 2023 doi:10.20944/preprints202311.1736.v1



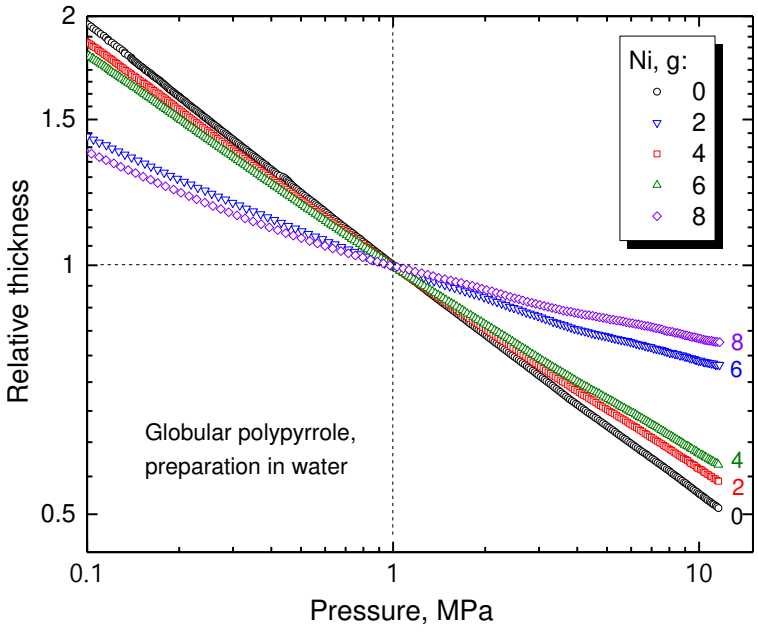


**Figure 8.** Pressure dependence of sample thickness relative to the thickness at 1 MPa for various contents of nickel.

*3.6. Magnetic Properties*

The magnetization curves reflect the properties of nickel (Figure 9). The saturation magnetization increased with nickel content (Table 2). As expected, polypyrrole does not contribute to magnetic properties and, consequently, its morphology has no effect.

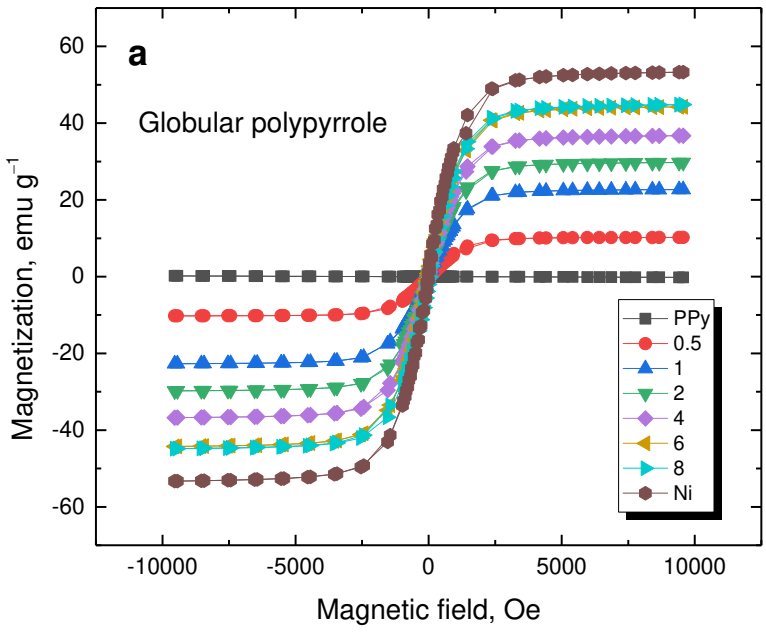

Preprints (www.preprints.org) | NOT PEER-REVIEWED | Posted: 28 November 2023 doi:10.20944/preprints202311.1736.v1



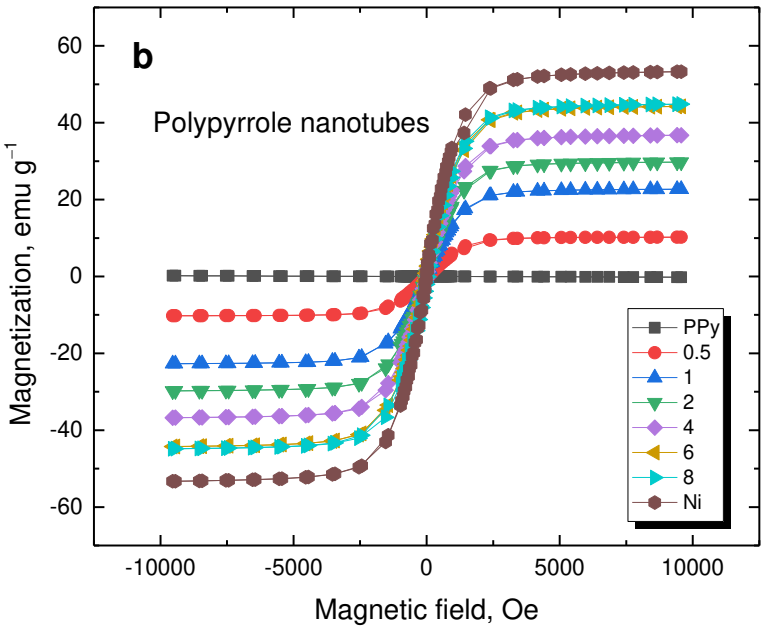


**Figure 9.** Magnetization curves of (a) globular polypyrrole and (b) polypyrrole nanotubes deposited on various amounts of nickel microparticles (in g).

**Table 2.** Coercivity, $H_C$, remanent magnetization, $M_R$, and saturation magnetization, $M_S$, of polypyrrole composites prepared with various amount of nickel, *Ni* in water.

| ***Ni*, g** | **$H_C$, Oe** | **$M_R$, emu g$^{-1}$** | **$M_S$, emu g$^{-1}$** |
|---|---|---|---|
| Globular polypyrrole | | | |
| 0.5 | 38.0 | 1.78 | 10.2 |
| 1 | 39.0 | 5.47 | 22.7 |
| 2 | 39.4 | 1.14 | 29.7 |
| 4 | 39.6 | 1.85 | 36.7 |
| 6 | 39.7 | 0.02 | 44.2 |
| 8 | 40.1 | 2.04 | 44.8 |
| Polypyrrole nanotubes | | | |
| 0.5 | 38.9 | 2.26 | 11.7 |
| 1 | 38.5 | 4.87 | 15.3 |
| 2 | 38.8 | 7.19 | 17.6 |
| 4 | 39.9 | 1.48 | 28.7 |
| 6 | 40.3 | 2.00 | 39.3 |
| 8 | 40.2 | 3.82 | 44.3 |
| Nickel | | | |
| Ni | 41.7 | 0.2 | 53.3 |

*3.7. Magnetorheology*

Due to the magnetic properties afforded by nickel, the composites can be tested in the design of magnetorheological fluids which are suspensions composed of magnetic micron-sized particles and a non-magnetic liquid phase [30]. Viscosity of these suspensions can be increased several orders of magnitude in a less than a second when an external magnetic field is applied. Due to the density mismatch of the particles and the carrier these systems suffer from sedimentation instability. Coating the particles is one of the most common solutions [31]. The coating on nickel microparticles with organic polymer, polypyrrole, reduces the average density of composite particles and thus prevents

Preprints (www.preprints.org) | NOT PEER-REVIEWED | Posted: 28 November 2023 doi:10.20944/preprints202311.1736.v1



the sedimentation of solid phase [32,33]. The systems incorporating nickel have been reported seldom [34]. It has been observed that the magnetorheological effect depended on the morphology [35] and particle size [36] of dispersed phase. The coating of nickel particles with polypyrrole reported in present study may also be regarded as a way how to alter the properties of dispersed phase.

The flow curves of the composite prepared with 8 g of nickel (= 83.2 wt% Ni, Table 1) are shown in Figure 10. The shear stress increased with the intensity of the magnetic field up to 450 kA $m^{-1}$. Then the particles were magnetically saturated (as showed in the magnetization curves) and the shear stress remains at approximately the same level. For the majority of the experimental window, the stress increased more than 10 times. A Bingham plastic behaviour was observed during the on-state. The particles form chain-like structures granting the fluid a yield stress. However, above shear rate of 1 $s^{-1}$, the hydrodynamic forces started to compete with magnetostatic ones, eventually overtaking them. During the off-state below the shear rate of 10 $s^{-1}$, a flow instability was observed, a result of shear banding. This is a common behaviour for certain colloids especially when a plate–plate geometry is used. The selection of this geometry, however, is key for a uniform magnetic field. A dotted line has been drawn following the behaviour at high shear rates for comparison in case there was no shear banding.

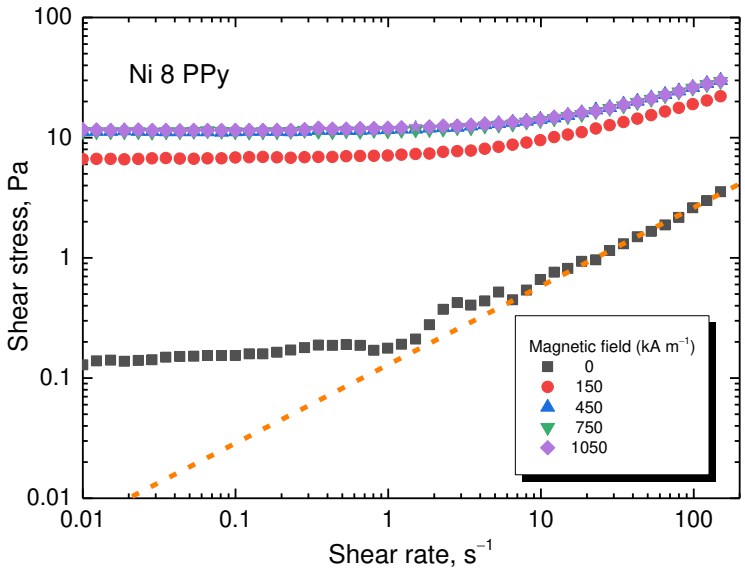


**Figure 10.** Flow curves at various magnetic fields for the composite prepared with 8 g of nickel. The dashed line represents the potential flow curve during the off-state if shear band were not present.

The flow curves for the sample using the lowest 2 g content of nickel in the reaction mixture (= 56.4 wt% Ni, Table 1), can be seen in Figure 11a. When a magnetic field was applied, the shear stress significantly increased with the trend being similarly to the sample shown in Figure 10. However, the shear stress increase is lower for the sample with low nickel content due to the lower content of magnetic component. The same instabilities were observed (Figure 11b). However, for repetitions of the flow curves, a behaviour closer to reality is found, with the data not forming an unstable plateau. The data at lower shear rates are scattered due to the low torque measured by the instrument, nevertheless, the trend is clear.

Preprints (www.preprints.org) | NOT PEER-REVIEWED | Posted: 28 November 2023 doi:10.20944/preprints202311.1736.v1



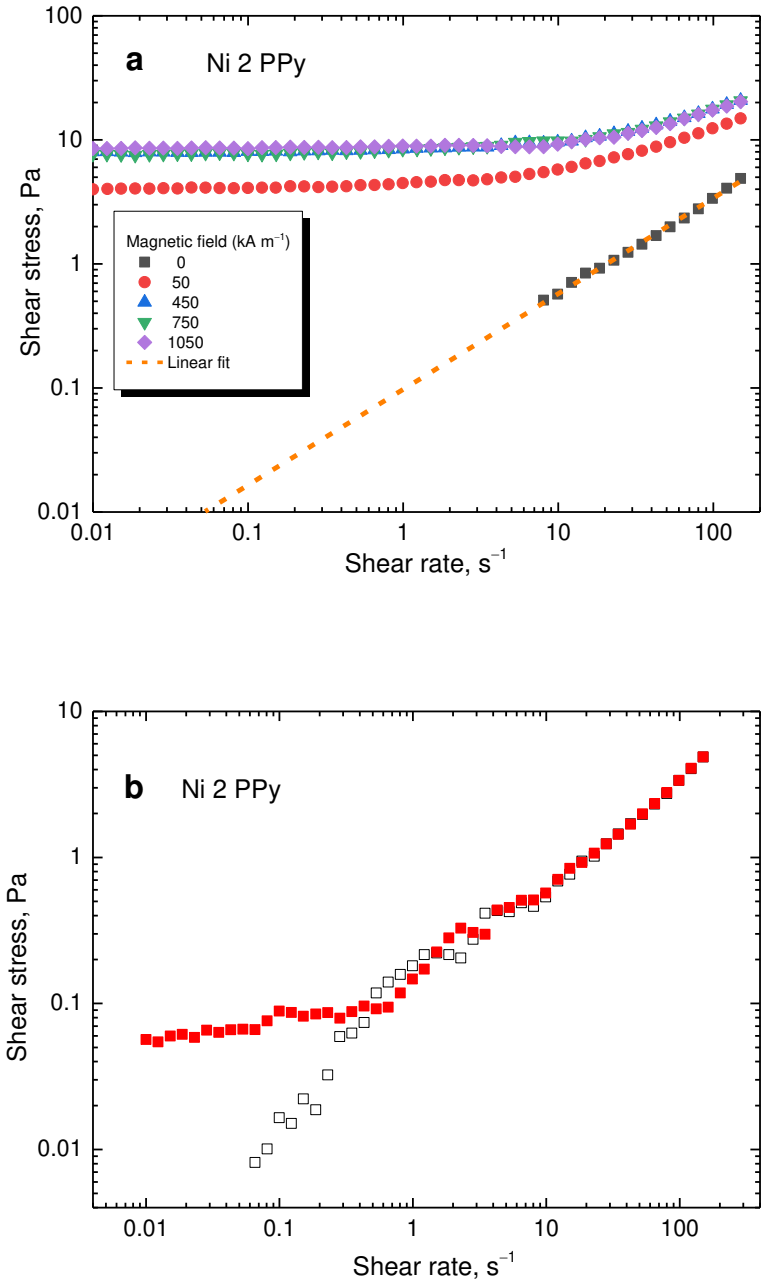


**Figure 11.** (a) Flow curves at various magnetic fields for the lowest 2 g nickel content. The dotted line represents a potential flow curve during the off-state if shear band was not present. (b) Flow curves during the off-state. The full squares depict data with shear banding present while open squares those without shear banding.

Furthermore, both tested samples were exposed to a steady shear rate of 50 $s^{-1}$ with the magnetic field turned on and off every 20 s and gradually increasing level (Figure 12a). The stress increased immediately after the magnetic field was applied. When the magnetic field was turned off, the stress reached its original values showing great control. The sample with high 8 g nickel content showed both lower off-state and higher on-state stress promoting it as a better candidate for applications regarding magnetorheology. The average stress of the on- and off-states were calculated for both samples and the magnetorheological performance was obtained by dividing the on-state stress by the off-state (Figure 12b). The sample with 8 g nickel had approximately three times higher performance while, for both samples above 450 kA $m^{-1}$, the performance remains the same as the nickel particles

Preprints (www.preprints.org) | NOT PEER-REVIEWED | Posted: 28 November 2023 doi:10.20944/preprints202311.1736.v1



are magnetically saturated. It is important to note, that there was a nickel based magnetorheological fluid with a similar carrier [34]. Present composite particles have nearly two times higher performance with only 9 wt% loading while the compared system [34] used 60 wt% particles.

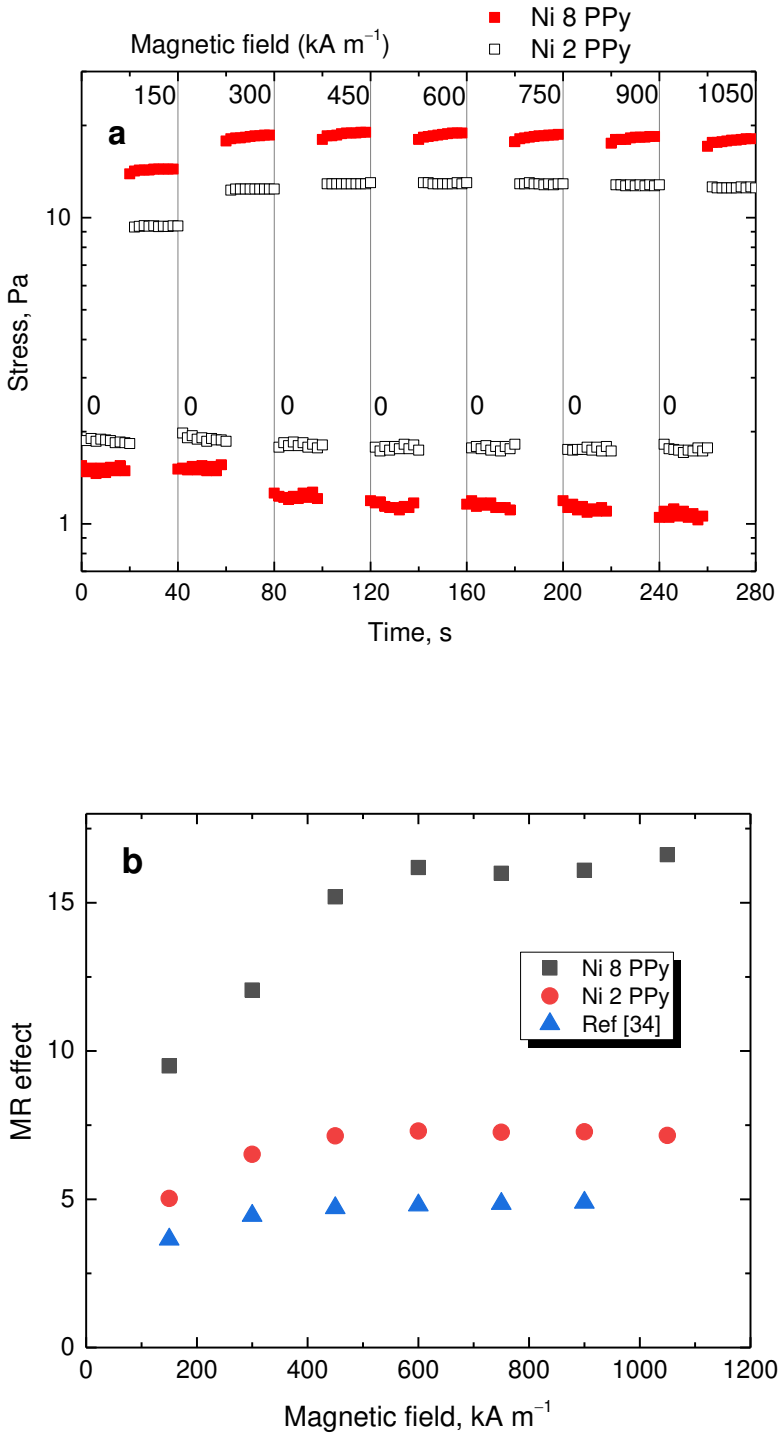


**Figure 12.** (a) Step-wise increase in magnetic field under shear rate of 50 s$^{-1}$ for samples prepared with 8 g (full squares) and 2 g nickel (open squares). (b) The magnetorheological performance as a function of magnetic field.

## 4. Conclusions

The hybrid organic/inorganic composites displaying electrical conductivity and magnetic properties, polypyrrole-coated nickel microparticles, have been prepared and characterized. While the oxidation of pyrrole with iron(III) chloride in the presence of nickel does not provide desired composites due to metal dissolution, the use of ammonium peroxydisulfate does. Resistivity of composite powders has been newly determined as a function of applied pressure. The conductivity measured on pellets was of the order of $10^{-1}$ S $cm^{-1}$, i.e. slightly lower than that of neat polypyrrole. Electrical properties did not depend on the polypyrrole morphology, globules or nanotubes, or acidity of reaction medium. The conductivity of nickel did not contribute to the overall conductivity of composites, which was determined only by polypyrrole matrix. In fact, the conductivity moderately decreased with increasing content of well-conducting nickel. This apparent paradox is explained by the inability of nickel cores to produce conducting pathways as they are always separated by polypyrrole coating. Magnetic properties are independent of polypyrrole content and morphology, and the magnetization is proportional to the nickel content. The hybrid composites of this type may find application as competitive functional materials, e.g., in magnetorheology as illustrated by present results.

**Author Contributions:** Marek Jurča: Synthesis, Writing – review & editing. Jarmila Vilčáková: Formal analysis. Natalia E. Kazantseva: Validation. Andrei Munteanu: Investigation, Writing – review & editing. Lenka Munteanu: Data Curation. Michal Sedlačík: Supervision, Funding acquisition, Resources. Jaroslav Stejskal: Conceptualization, Writing – original draft. Miroslava Trchová: Investigation, Data curation. Jan Prokeš: Investigation, Validation.

**Funding:** The authors thank the Czech Science Foundation (A.M., M.S., L.M.: 23-07244S and J.S.: 22-25734S) for financial support.

**Conflicts of Interest:** The authors declare no conflict of interest.

## References

1. Obodo, RM; Shinde, NM; Chime, UK; Ezugwu, S; Nwanya, AC; Ahmad, S; Maaza, M; Ejikeme, PM; Ezema, FI. Recent advances in metal oxide/hydroxide on three-dimensional nickel foam substrate for high performance pseudocapacitive electrodes. Curr. Opinion Electrochem. 2020, 21, 242–249. DOI: 10.1016/j.coelec.2020.02.022
2. Ul-Hoque, MI; Holze, R. Intrinsically conducting polymer composites as active masses in supercapacitors. Polymers 2023, 15, 730. DOI: 10.3390/polym15030730.
3. Irshad, MS; Arshad, N; Wang, XB; Li, HR; Javed, MQ; Xu, Y; Alshahrani, LA; Mei, T; Li, JH. Intensifying solar interfacial heat accumulation for clean water generation excluding heavy metal ions and oil emulsions. Solar RRL 2021, 5, 2100427. DOI: 10.1002/solr.202100427
4. Ghanbari, R; Ghorbani, SR. High-performance nickel molybdate/reduced graphene oxide/polypyrrole ternary nanocomposite as flexible all-solid-state asymmetric supercapacitor. J. Energy Storage 2023, 60, 106670. DOI: 10.1016/j.est.2023.106670
5. Shi, AR; Song, XM; Wei, L; Ma, HY; Pang, HJ; Li, WW; Liu, XW; Tan, LC. Design of an internal/external bicontinuous conductive network for high-performance asymmetrical supercapacitors. Molecules 2023, 27, 8168. DOI: 10.3390/molecules27238168
6. Stejskal, J. Conducting polymer-silver composites. Chem. Pap. 2013, 67, 814–848. DOI: 10.2478/s11696-012-0304-6
7. Wei, JT; Xing, GZ; Gao, L; Suo, H; He, XP; Zhao, C; Li, S; Xing, SX. Nickel foam based polypyrrole-Ag composite film: a new route toward stable electrodes for supercapacitors. New J. Chem. 2020, 37, 337–341. DOI: 10.1039/c2nj40590c
8. Gao, J; Wang, XH; Wang, XQ; Que, RH; Fang, Y; Shi, B; Wang, ZH. Hierarchical polypyrrole/$Ni_3S_2$@$MoS_2$ core-shell nanostructures on a nickel foam for high-performance supercapacitors. RSC Adv. 2016, 6, 68460–68467. DOI: 10.1039/c6ra12095d
9. Hasanzadeh, M; Ansari, R; Farahpour, M. Cobalt disulfide/polypyrrole cauliflower-like nanocomposite: Single-pot hydrothermal synthesis, characterization, and their enhanced storage energy in supercapacitors. J. Alloy Compd. 2023, 951, 169965. DOI: 10.1016/j.jallcom.2023.169965
10. Wang, S; Fan, YK; Wang, F; Su, YN; Zhou, X; Zhu, ZQ; Sun, HX; Liang, WD; Li, A. Potentially scalable fabrication of salt-rejection evaporator based on electrogenerated polypyrrole-coated nickel foam for efficient solar steam generation. Desalination 2021, 505, 114982. DOI: 10.1016/j.desal.2021.114982

11. Karazehir, T. Electrodeposited Pd nanoparticles on polypyrrole/nickel foam for efficient methanol oxidation. Int. J. Hydrogen Energy 2023, 48, 10493–10506. DOI: 10.1016/j.ijhydene.2022.12.059
12. Yu, HB; Che, M; Zhao, B; Lu, Y; Zhu, SY; Wang, XH; Qin, WC; Huo, MX. Enhanced electrosorption of rhodamine B over porous copper-nickel foam electrodes modified with graphene oxide/polypyrrole. Synth. Met. 2021, 262, 116332. DOI: 10.1016/j.synthmet.2020.116332
13. Ren, J; Shen, M; Li, ZL; Yang, CM; Liang, Y; Wang, HE; Li, JH; Li, N; Qian, D. Towards high-performance all-solid-state asymmetric supercapacitors: A hierarchical doughnut-like $Ni_3S_2$@PPy core-shell heterostructure on nickel foam electrode and density functional theory calculations. J. Power Sources 2021, 501, 230003. DOI: 10.1016/j.jpowsour.2021.230003
14. Song, YC; Hong, PD; Li, TF; Ma, GX; Deng, QH; Zhou, YM; Zhang, YW. A nanoflower-like polypyrrole-based cobalt-nickel sulfide hybrid heterostructures with electrons migration to boost overall water splitting. J. Colloid Interface Sci. 2022, 618, 1–10. DOI: 10.1016/j.jcis.2022.03.035
15. Li, J; Zou, YJ; Li, B; Xu, F; Chu, HL; Qiu, SJ; Zhang, J; Sun, LX; Xiang, CL. Polypyrrole-wrapped $NiCo_2S_4$ nanoneedles as an electrode material for supercapacitor applications. Ceramics Int. 2021, 47, 16562–16569. DOI: 10.1016/j.ceramint.2021.02.227
16. Shen, XJ; Wei, XY; Wang, TF; Li, SM; Li, HT. Polypyrrole embedded in nickel-cobalt sulfide nanosheets grown on nickel particles passivated silicon nanowire arrays for high-performance supercapacitors. Chem. Eng. J. 2023, 461, 141745. DOI: 10.1016/j.cej.2023.141745
17. Ashassi-Sorkhabi, H; Kazempour, A; Moradi-Alavian, S; Asghari, E; Lamb, JJ. 3D nanostructured nickel film supported to a conducting polymer as an electrocatalyst with exceptional properties for hydrogen evolution reaction. Int. J. Hydrogen Energy 2023, 48, 29865–29876. DOI: 10.1016/j.ijhydene.2023.04.139
18. Jiao, FZ; Wu, J; Zhang, TT; Pan, RJ; Wang, ZH; Yu, ZZ); Qu, J. Simultaneous solar-thermal desalination and catalytic degradation of wastewater containing both salt ions and organic contaminants. ACS Appl. Mater. Interfaces 2023, 15, 41007–41018. DOI: 10.1021/acsami.3c09346
19. Oriňáková, R; Filkusová, M. Hydrogen evolution on microstrutured polypyrrole films modified with nickel. Synth. Met. 2010, 160, 927–931. DOI: 10.1016/j.synthmet.2010.02.002
20. Chemchoub, S; Oularbi, L; El Attar, A ; Younssi, SA; Bentiss, F; Jama, C; El Rhazi, M. Cost-effective non-noble metal supported on conducting polymer composite such as nickel nanoparticles/polypyrrole as efficient anode electrocatalyst for ethanol oxidation. Mater. Chem. Phys. 2020, 250, 123009. DOI: 10.1016/j.matchemphys.2020.123009
21. Emir, G; Dilgin, Y; Ramanaviciene, A; Ramanavicius, A. Amperometric nonenzymatic glucose biosensor based on graphite rod electrode modified by Ni-nanoparticle/polypyrrole composite, Microchem. J. 2021, 161, 105751. DOI: 10.1016/j.microc.2020.105751
22. Šišoláková, I; Gorejová, R; Chovancová, F; Shepa, J; Ngwabebhoh, FA; Fedorková, AS; Sáha, P; Oriňáková, R. Polymer-based electrochemical sensor: Fast, accurate, and simple insulin diagnostics tool. Electrocatalysis 2023, 14, 697–707. DOI: 10.1007/s12678-023-00827-w
23. Genetti, WB; Yuan, WL; Grady, BP; O'Rear, EA; Lai, CL; Glatzhofer, DT. Polymer matrix composites: Conductivity enhancement through polypyrrole coating of nickel flake. J. Mater. Sci. 1998, 33, 3085–3093. DOI: 10.1023/A:1004387621165
24. Stejskal, J; Acharya, U; Bober, P; Hajná, M; Trchová, M; Mičušík, M; Omastová, M; Pašti, I; Gavrilov, N. Surface modification of tungsten disulfide with polypyrrole for enhancement of the conductivity and its impact on hydrogen evolution reaction. Appl. Surf. Sci. 2019, 492, 497–503. DOI: 10.1016/j.apsusc.2019.06.175
25. Jurča, M; Vilčáková, J; Kazantseva, NE; Prokeš, J; Trchová, M; Stejskal, J. Conducting and magnetic hybrid polyaniline/nickel composites. Synth. Met. 2022, 291, 117165. DOI: 10.1016/j.synthmet.2022.117165
26. Stejskal, J; Trchová, M. Conducting polypyrrole nanotubes: a review. Chem. Pap. 2018, 72, 1563–1595. DOI: 10.1007/s11696-018-0394-x
27. Stejskal J; Vilčáková J; Jurča M; Fei HJ; Trchová M; Kolská Z; Prokeš J; Křivka I. Polypyrrole-coated melamine sponge as a precursor for conducting macroporous nitrogen nitrogen-containing carbons. Coatings 2022, 12, 324. doi: 10.3390/coatings12030324
28. Cascales, JJL; Fernandez, AJ; Otero, TF. Characterization of the reduced and oxidized polypyrrole/water interface: A molecular dynamics simulation study. J Phys. Chem. B 2003, 107, 9339–9343. DOI: 10.1021/jp027717o
29. Trchová, M.; Stejskal, J. Resonance Raman spectroscopy of conducting polypyrrole nanotubes: Disordered surface versus ordered body. J. Phys. Chem. A 2018, 122, 9298−9306. DOI: 10.1021/acs.jpca.8b09794
30. Park, BJ; Fang, FF; Choi, HJ. Magnetorheology: materials and application. Soft Matter 2010, 6, 5246–5253. DOI: 10.1039/C0SM00014K
31. Ronzova, A; Sedlacik, M; Cvek, M. Magnetorheological fluids based on core-shell carbonyl iron particles modified by various organosilanes: synthesis, stability and performance. Soft Matter 2021, 17, 1299–1306. DOI: 10.1039/d0sm01785j

32. Mrlik, M; Sedlacik, M; Pavlinek, V; Peer, P; Filip, P; Saha, P. Magnetorheology of carbonyl iron particles coated with polypyrrole ribbons: The steady shear study. J. Phys.: Conf. Ser., 2013, 412, 1–7. DOI: 10.1088/1742-6596/412/1/012016
33. Munteanu, A; Plachý, T; Munteanu, L; Ngwabebhoh, FA; Stejskal, J; Trchová, M; Kubík, M ; Sedlačík, M. Bidisperse magnetorheological fluids utilizing composite polypyrrole nanotubes/magnetite nanoparticles and carbonyl iron microspheres. Rheol. Acta 2023, 62, 461–472. DOI: 10.1007/s00397-023-01409-9
34. Munteanu, L; Masař, M; Sedlačík, M; Kohl, M; Kalendová, A. Magneto-active ferrite-based paint pigments. AIP Conf. Proc. 2023, 2997, 040006. DOI: 10.1063/5.0159567
35. Morillas, JR; Carreón-González, E; de Vicente, J. Effect of particle aspect ratio in magnetorheology. Smart Mater. Struct. 2015, 24, 125005. DOI: 10.1088/0964-1726/24/12/125005
36. Gwon, H; Park, S; Lu, Q; Choi, HJ; Lee, S. Size effect of iron oxide nanorods with controlled aspect ratio on magneto-responsive behavior. J. Ind. Eng. Chem. 2023, 124, 279–286. DOI: 10.1016/j.jiec.2023.04.017